Iranian Polymer Journal (2023) 32:887–896
https://doi.org/10.1007/s13726-023-01171-y

ORIGINAL RESEARCH

Torsional behavior of glass fiber-reinforced polymer composite: polymer matrix effect and acoustic emission signal analysis

Abburi Lakshman Kumar[1] · **M. Prakash**[1]

Received: 17 November 2022 / Accepted: 5 March 2023 / Published online: 29 March 2023

Abstract

The influence of polymer matrix on torsional rigidity of glass fiber-reinforced polymer (GFRP) composite rods was monitored using acoustic emission (AE) analysis. The GFRP composite rods employed in this work were fabricated by vacuum-assisted resin transfer molding (VARTM) method with two different polymer matrices (i.e., LY556 epoxy resin and Aquabond 520 epoxy). The torsional tests were performed using a static torsion machine, and the AE analysis was used to monitor the physical discontinuities initiated during the test. The fast Fourier transform (FFT) and discrete wavelet packet transform (DWPT) methods were used to analyze the AE signals and to measure the resonance frequency in various failure events. Subsequently, all the damages resulting from fiber–matrix debonding, fiber failure and fiber breaking could be recognized through AE signals. From the FFT method, different failures were observed in LY556 epoxy matrix in frequencies of 85.459, 141.168 and 300.329 kHz. In case of Aquabond 520 matrix, the frequencies were observed at 48.834, 87.90 and 302.77 kHz, indicating, that the failure occurred in the mode of matrix cracking, debonding and fiber fracture, respectively. The FFT failures frequencies were consistent with the DWPT (discrete wavelet packet transform) frequency bands. The correlation between the failure and AE signals was obtained by analyzing the fractography taken by scanning electron microscopy (SEM).

✉ M. Prakash
prakashmuniyandi@gmail.com

[1] Department of Mechanical Engineering, SRM Institute of Science and Technology, Kattankulathur, Chennai, India

Graphical abstract

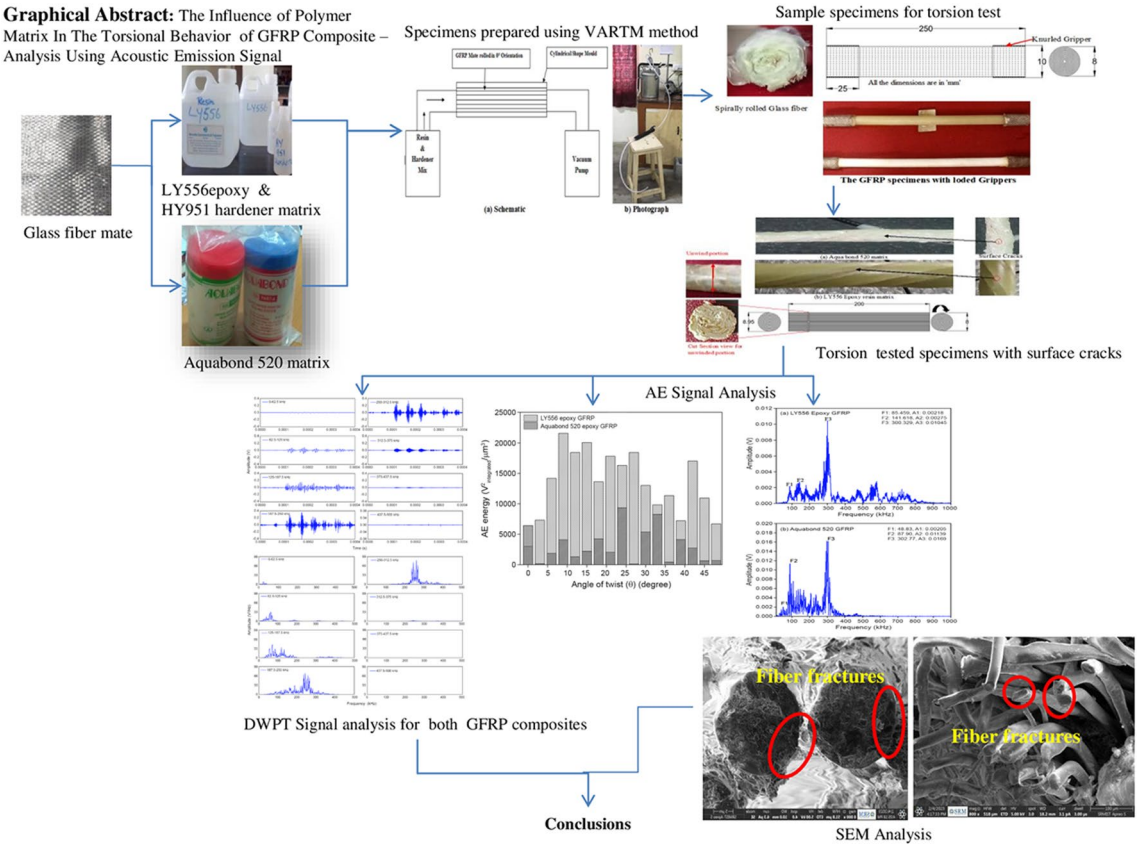

Keywords Acoustic emission · Fast Fourier transform · Torsional test · Resonance frequency · Fractography

Introduction

Composite materials are widely used in automobile, aerospace, and civil structures due to their advantages of light density and high specific strength-to-weight ratio. Particularly, in automobiles, the efficiency of the vehicle is greatly lost due to the increased weight of rotating metal parts such as the torsional bar and stabilizing bars. These power losses can be reduced with the use of fiber-reinforced composites [1–3]. The need for improving the performance of composite structures in automobile industries is addressed by the study of fatigue analysis under multiaxial and uniaxial loadings [4]. Waste textile and Aramid fibers with nanocomposites are also used to develop hybrid composites to reduce the weight of automobile parts and to develop environmental friendly composites [5, 6]. The torsional strength is an essential mechanical property in composite rods that is challenging to achieve.

Many researchers have analyzed composite rods and shafts, and several numerical and experimental studies have been performed in earlier research studies. Talib et al. [7] developed hybrid carbon/glass FRP (fiber-reinforced polymer) driving shafts for studying buckling torque, lateral bending natural frequency, and torsional frequency for different layers and fiber orientations. The obtained experimental results were compared with FEM (finite-element method) results and it was observed that the stacking sequence had an effect on fatigue behavior. The properties of the hybrid composite were noted to vary when compared with the properties of a single polymer composite. Sevkat et al. [8] studied the residual properties of carbon-glass/epoxy hybrid composite shaft subjected to impact loading experimentally and numerically. The energy absorption ability of glass-reinforced shaft was best and the damage induced by the impacts reduced the torsional strength. Hybridization had an effect on torsional strength and energy [9]. Capela et al. [10] studied the fatigue strength of carbon fiber-reinforced polymer (CFRP) tubes under biaxial bending/torsional dynamic loadings. The authors found that the fatigue strength was reduced because of the combined torsional stress and bending load stress. With combined loadings like that of biaxial or uniaxial loading, the fatigue strength of shaft or rods tends

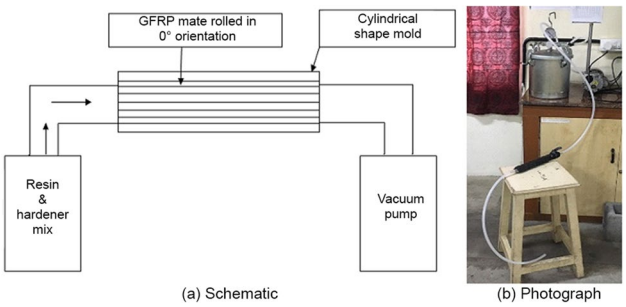

Fig. 1 VARTM (vacuum-assisted resin transfer mold) method setup

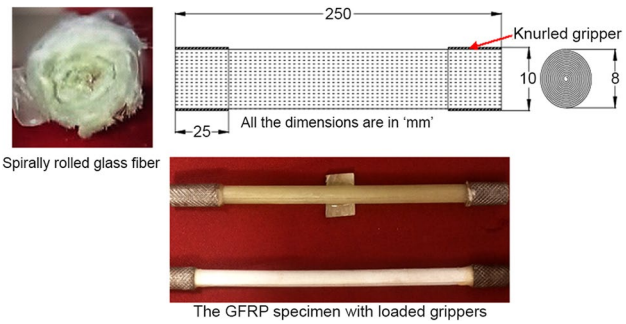

Fig. 2 The schematic and pictorial view of fabricated specimens

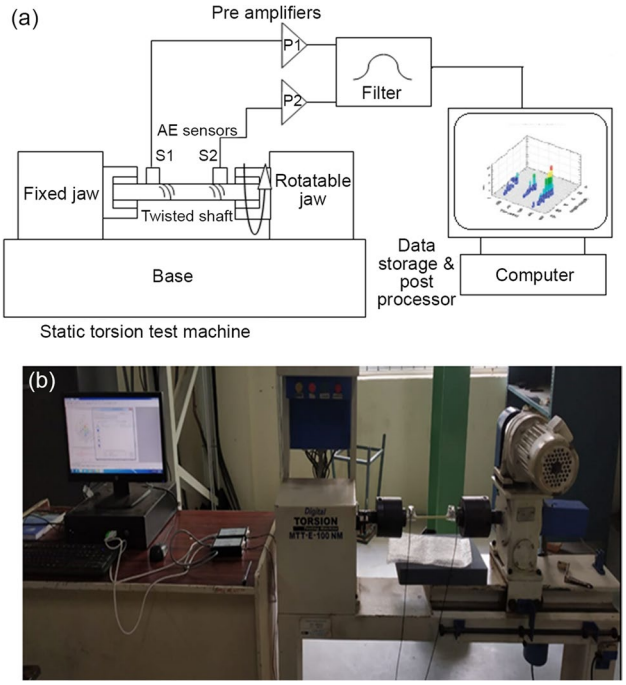

Fig. 3 Experimental setup of physical and schematic layout

to drop. In the study conducted by Tasdelenet et al. [11], vacuum-assisted resin transfer molding (VARTM) and vacuum bagging methods were used to prepare two composite shafts to study their torsional strength. From the results, it was identified that the torsional strength varied depending on the fabrication method. Tariq et al. [12] studied the effect of hybrid reinforcement by examining the torsional strength of hollow shafts manufactured using two different methods such as vacuum bagging method and VARTM method in different lay-up sequences and different fiber orientations. The experimental results were evaluated with the help of finite-element analysis (FEA) results and it was observed that the specimens fabricated by VARTM method showed good torsional strength.

Non-destructive testing techniques are commonly used to monitor different failure mechanisms such as fiber breakage, fiber–matrix debonding, and fiber pull-outs. The acoustic emission method is extensively used for the study and analysis of micro- and macro-cracks of all materials. Arumugam et al. [13] have used acoustic emission (AE) monitoring and artificial neural network (ANN) to predict the residual strength of post-impacted carbon/epoxy composite laminates. They found that AE combined with ANN was effective in predicting different failures. During curing, voids are likely to form in composite specimens under certain temperatures. Kakakasery et al. [14] have studied the effect of formation of a moderate number of voids in the composite structure using AE technique. They observed that the void formation led to failure in CFRP laminates and studied the failure mechanism. Kossmann et al. [15] have adopted the acoustic emission method to study the effect of voids in GFRP laminates on their damage behavior under compression loading. By separation of AE frequency bands and their amplitude, and using energy levels, it is easy to find the types of failures in laminated composites. The AE technique is a good tool that can be utilized to detect micro- and macro-voids. The AE signals produced by the sensors are collected and then processed using different methods. Roundi et al. [16] performed static and fatigue tensile tests on glass/epoxy composite laminates. The damage propagation during the test was monitored by acoustic emission method in online mode. The k-means method and principal component method (PCA) are used for signal processing. In these methods, the signals are divided into four levels which are then matched with the failure of laminates. Most researchers who have studied the failure modes in laminates have adopted the AE method. The same AE method can also be used to study torsional failures in composite shafts and solid rods. Hao et al. [17] studied the torsional strength of 3D braided composite shafts using the acoustic emission method. The gradual damages were identified by the frequency of AE signals for different braiding angle fiber orientations. Most researchers in this field have studied torsional failure hollow shafts, fabricated by filament winding method and solid rods, manufactured using pultrusion method. The

failure is monitored by AE method while, the signals are analyzed using a simple wavelet method.

Very few researchers have studied the torsional strength of solid rods, so that in this work, an attempt is made to study the effect of spirally stacked reinforcement and the influence of matrix materials in torsional behavior. The damage propagation during the torsional test is monitored using AE analysis in different polymer matrices of GFRP rods. The composite rods were prepared by VARTM method. The torsional tests were performed using a static torsion machine. The AE signals were analyzed using the fast Fourier transform method. Discrete wavelet packet transform method was used to identify the AE frequency, amplitude, and energy signals of different levels.

Experimental

Two different types of polymer matrices were used in this study: LY556 resin and the curing hardener of HY951 with E-glass fiber, and Aquabond 520 epoxy with E-glass fiber. The tensile strength of LY556 matrix is 73.3 MPa, and for Aquabond 520 matrix, it is 24 MPa, and the modulus of LY556 matrix is 3470 MPa, and for Aquabond 520 matrix, it is 1800 MPa. All the specimens were fabricated using vacuum-assisted resin transfer molding (VARTM) method, in which initially the E-glass fiber mat was spirally rolled, placed in an aluminum mold, and closed with simple bagging covered at the sides. While vacuum is created from one end of the mold at 10 MPa, the resin is fed from the other end of the mold. The schematic and pictorial views of fabrication method are shown in Fig. 1. The matrix preparation ratio of LY556 resin to curing hardener HY951 was 10:1 and the curing process was performed at room temperature for 24 h. For Aquabond 520, the ratio of 2:1 was maintained. The curing process was performed at room temperature for 12 h. The specimens were fabricated with 250 mm length, and the edges were smoothed using grit sand paper. The volume fraction of the fiber in specimens was maintained at 51–52%. The end gripping difficulties during the investigation of torsional properties of the composite rod were properly analyzed and rectified in order to obtain reliable results. Small cracks were generated on the surface due to the gripping pressure in the testing machine. This could be solved by metal grippers fixed at both the ends up to the gripping area in the composite rod. To overcome the slipping problem in the metal gripper, knurling surface was generated on the metal grippers. The gripper area of the composite rod was 25 mm at each end. After fixing the grippers to the composite rod with Araldite paste, the specimens were cured at room temperature for 6 h. The gripper-loaded specimens are shown in Fig. 2.

The fiber-reinforced polymer composites are anisotropic materials. In these GFRP composite materials, the stress distribution to the matrix and fiber is very complicated to find because of the anisotropic property. The static torsion tests were performed using a MTT-E-100 static and dynamic torsion test machine with a maximum 100 N.m torsion capacity. To identify the torsional failure of the GFRP composite, the entire testing process was monitored using two piezoelectric sensors. The frequency range of the sensor was 100 kHz–1 MHz, and it was placed at the end of the gauge length of the specimen. The amplitude of AE signals was in the range of 0–50 dB. Two AE sensors were placed in the corner of gauge length of the test specimen, as shown in Fig. 3. The AE signals were collected using AE win software with a sampling frequency of 20 MHz. The AE signals were analyzed in the time domain to identify the root mean square (AE_{RMS}) and AE energy, and in the frequency domain using the fast Fourier transform method. More than 11.3 million signals of data were collected for processing during the torsion test out of which 65,536 signals of data were selected to study the AE_{RMS} value and for the time domain analysis. A number of 8192 signals were selected as data to conduct experiments for FFT and DWPT

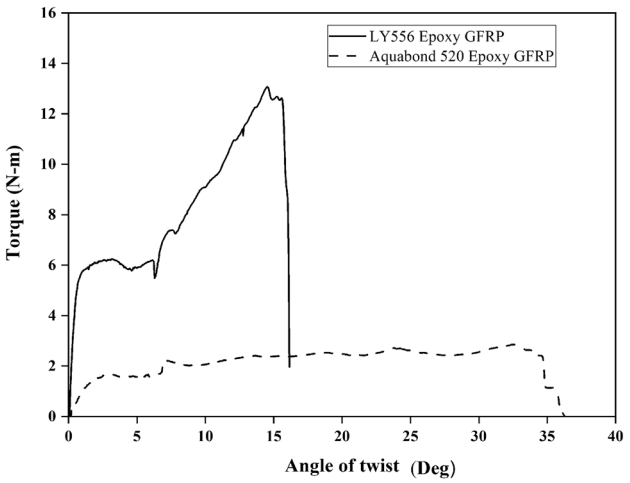

Fig. 4 Torque versus angle of twist curves

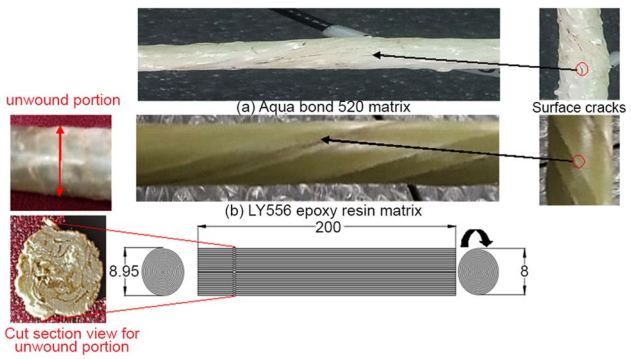

Fig. 5 Failures during torsion test: **a** LY556 epoxy GFRP, and **b** Aquabond 520 GFRP

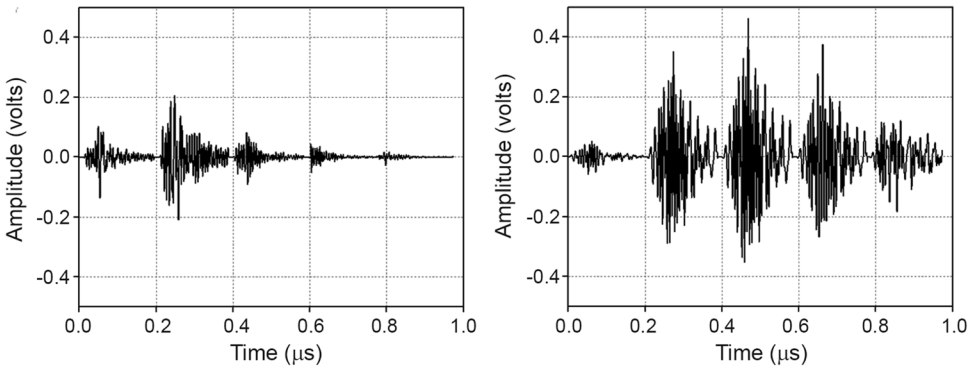

Fig. 6 AE signals for two different matrix materials

analysis [16]. The received AE signals were divided into 8 different frequency levels such as D1 (0–62.5 kHz), D2 (62.5–125 kHz), D3 (125–187.5 kHz), D4 (187.5–250 kHz), D5 (250–312.5 kHz), D6 (312.5–375 kHz), D7 (375–437.5 kHz) and D8 (437.5–500 kHz) with 3 dB bandwidth, using the DWPT algorithm of MATLAB® (R 2018). According to the Nyquist sampling theorem, twice the highest frequency was observed in the signal [19–21]. Therefore, the sampling frequency was fixed at 20 MHz in this case, and the frequency of the processed signals was taken to be as high as 500 kHz.

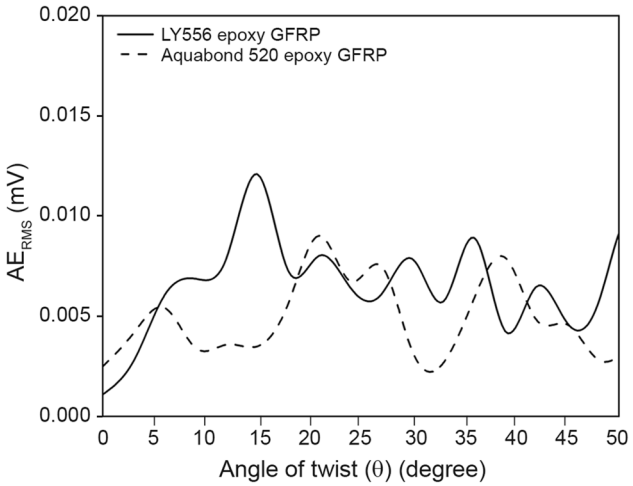

Fig. 7 Response graph AE RMS versus angle of twist

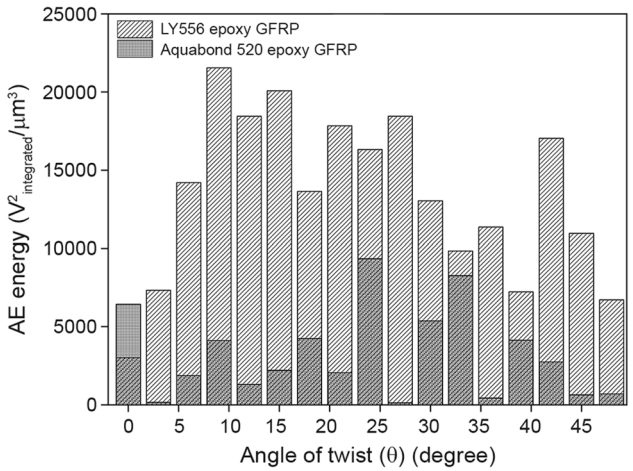

Fig. 8 AE energy versus angle of twist

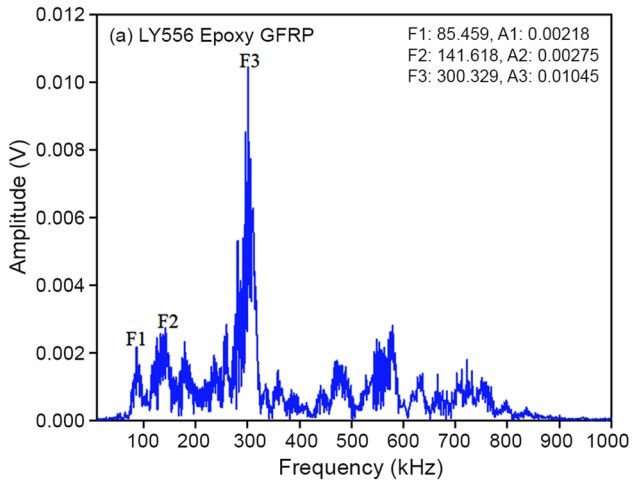

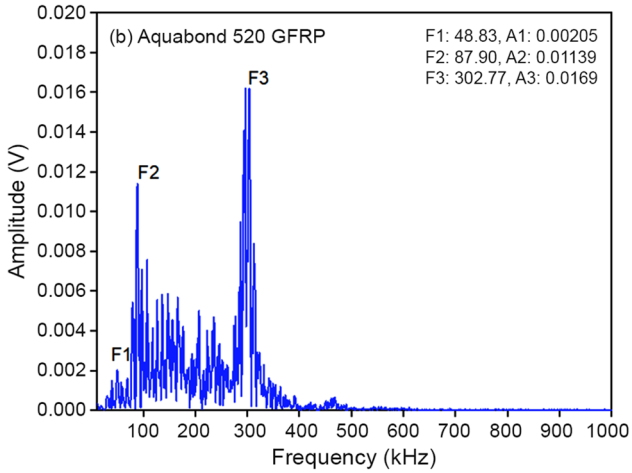

Fig. 9 FFT spectrum

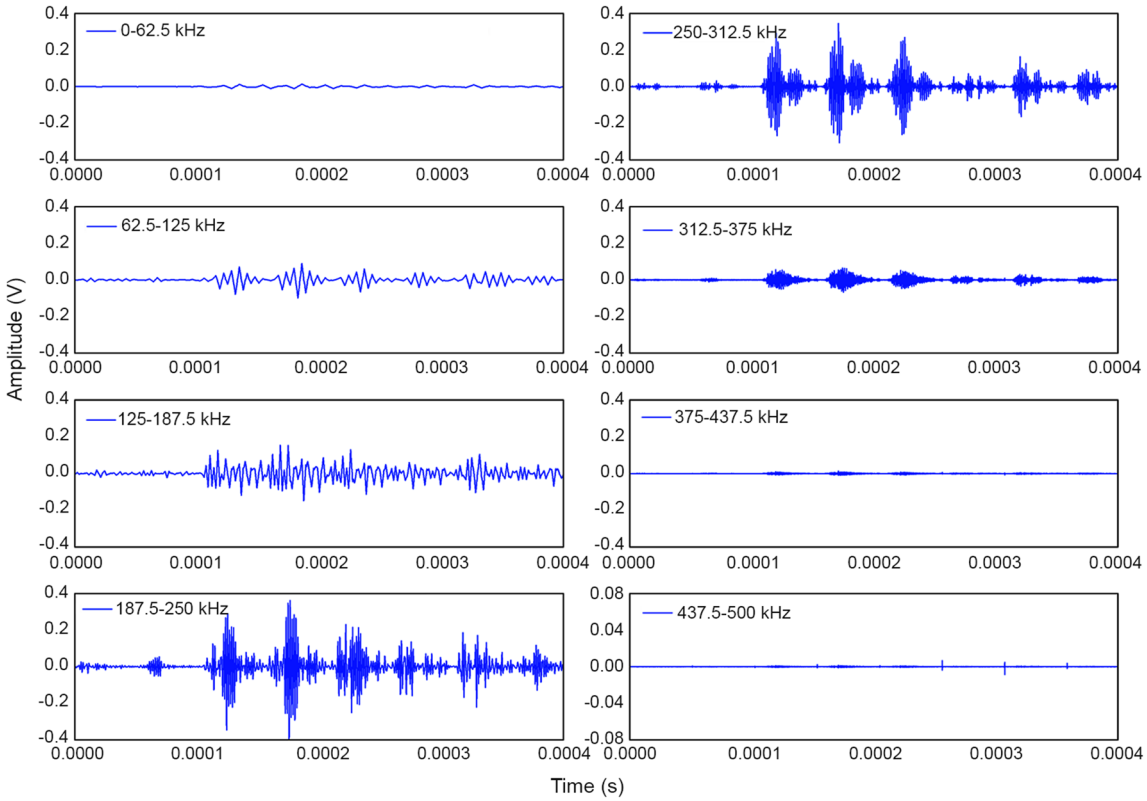

Fig. 10 Typical decomposed AE signals for Aquabond 520 epoxy GFRP

Results and discussion

The torque and angle of twist curves for different FRP composites are presented in Fig. 4. It is observed that, due to the elastic nature of the Aquabond 520, the related composite has a significantly less torque of 2.525 N.m with greater twist angle. However, for LY556 epoxy composite, the maximum torque is 13.5 N.m with the failure angle of 14.75°. The mechanical property of both materials is of linear elasticity. Catastrophic failure occurs and the load is suddenly decreased. Figure 5 shows the surface failure in different composites. When the load is applied, it is initially transferred to the matrix but after failure of matrix, the load is transferred to the fibers. The fiber mats are concentrically wounded along the axis of the composite rod. From Fig. 5, it is observed that while increasing the torsional load, one side of the fibers is wound in the fiber mat winding direction, while in the other side, the fibers are unwound. It causes matrix cracking and fiber–matrix debonding which may produce bulging before failure. The twisting of fiber occurs between the winding and unwinding in the direction along the axis of the rod, which leads to surface cracking (Fig. 5).

Figure 6 represents the AE signals obtained for the LY556 epoxy and Aquabond 520 matrix composites. These signals are based on time variance and amplitude. High-amplitude and high-variance peak signals are observed, especially in Aquabond 520 matrix, indicating the lack of bonding between the matrix and reinforcement. Studying its failure mechanism will be useful for the research community to determine appropriate applications. The characteristics of each failure mode are discussed from the time domain analysis and frequency domain analysis to calculate the root mean square and dominant frequency. The key details are analyzed with the application of the discrete wavelet packet transform (DWPT) method.

The AE_{RMS} versus angle of twist is shown in Fig. 7. For the LY556 epoxy resin matrix, the AE_{RMS} value is a high value of 0.013 mV in the twist angle range of 5°–15°, but for the Aquabond 520 epoxy, it is 0.009 mv in the twist angle range of 20°–25°.

Acoustic emission energy is also one measuring parameter to identify the different failures in fiber-reinforced polymer (FRP) materials. Figure 8 represents the AE energy at the angle of twist for different FRP composite materials. In this study, the maximum AE energy obtained is 23000

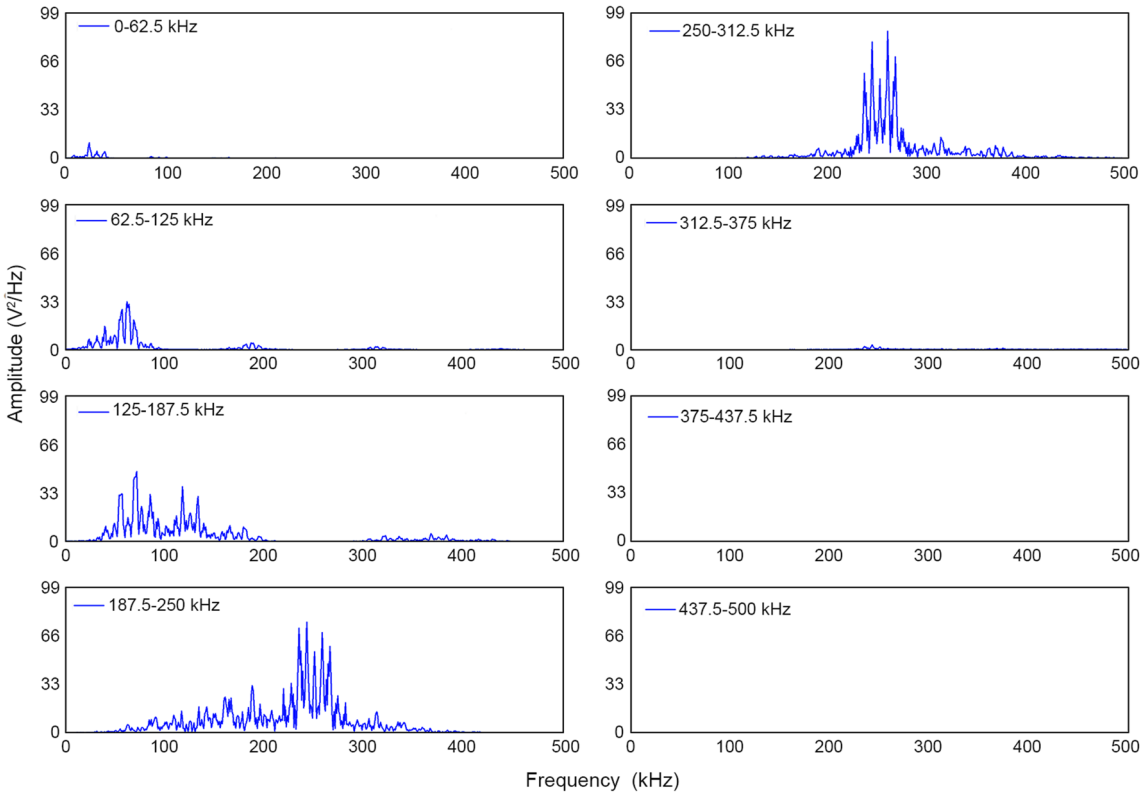

Fig. 11 Typical FFT of decomposed AE signals for Aquabond 520 epoxy GFRP

in 5°–15° twist angle range for LY556 epoxy GFRP, and for Aquabond 520 with GFRP material, it is 9800 in the angle of twist between 20° and 25°. When comparing the two, it is observed that the LY556 epoxy matrix receives more AE energy than the Aquabond 520 matrix. After reaching the maximum, the energy level gradually reduces in both the matrix materials, and the matrix failure continues [22].

The observed signals were processed using fast Fourier transform method and the results are shown in Fig. 9. The failure mode frequency of the AE signal for the Aquabond 520 matrix and LY556 matrix GFRP is identified from the peak frequency and named as F1, F2 and F3. From Fig. 9a, the frequency contents for the LY556 epoxy matrix are observed as: F1—85.459 kHz which represents the matrix failure, F2—141.168 kHz represents the debonding, and F3—300.329 kHz is associated with fiber breakage [18, 19, 23]. From Fig. 9b, it is noted that for Aquabond 520 matrix, F1—48.834 kHz represents the matrix cracking, F2—87.901 kHz for the matrix debonding, and F3—302.77 kHz indicates for the fiber failure [17, 18, 20].

For a detailed study of different failure frequency bands, the DWPT method is used and FFT peak frequency signals are matched with the DWPT frequency band for the identification of the various failure modes.

The DWPT method is used to identify and analyze the different failure amplitudes and frequency ranges over time for both matrix GFRP composites. The results of the decomposition of AE signals are shown in Figs. 10 and 11.

The DWPT frequency bands are divided into two groups, i.e., low-level bands and high-level bands based on their amplitude level. D2, D3, D4, D5 and D6 are found to represent the high-amplitude frequency bands, whereas D1, D7, and D8 indicate the low-level frequency bands. From FFT, the same trend of frequency and amplitude level is observed in LY556 matrix with F1, F2 and F3 frequency signals coming under high-level amplitude frequency bands such as D2, D3, D4, D5 and D6. In the Aquabond 520 matrix, the F1 frequency signals are observed in low-level frequency bands like D1, because of the more elastic nature of Aquabond 520 matrix, but the debonding and fiber failure (F2 and F3) frequencies are observed in high-level frequency bands such as D2 and D5.

Figure 11 illustrates the typical FFT signal for Aquabond 520 matrix, indicating that the FFT of the decomposed signal falls within the accepted range.

Figure 12 shows the fractography of the torsional failure of LY556 epoxy matrix and Aquabond 520 epoxy matrix GFRP composite materials, which represent

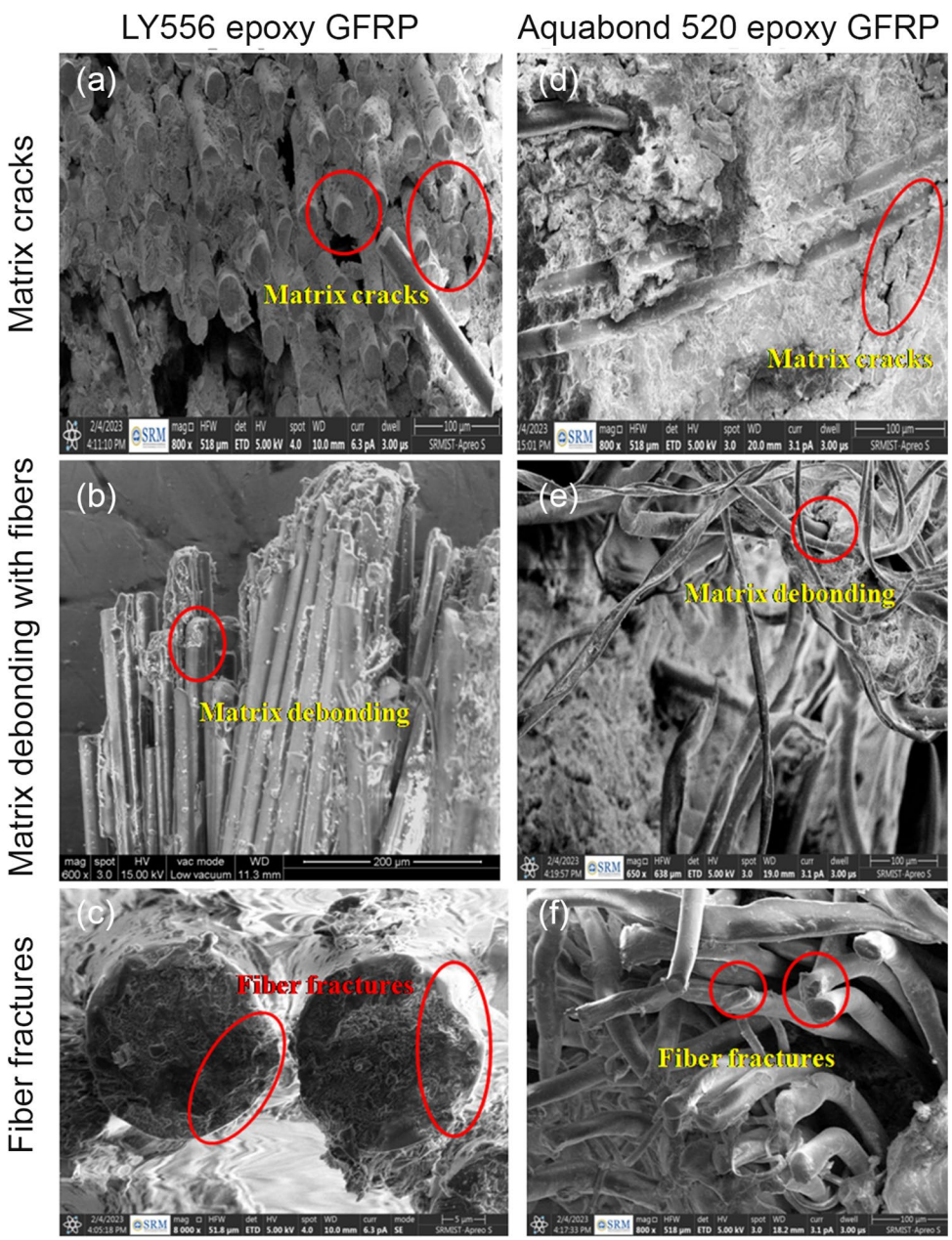

Fig. 12 Fractography of torsional failure

different failures such as matrix failure, debonding and fiber fracture. Figure 12a and d shows the matrix failures of both GFRP composites, from that it may be observed more matrix fracture in LY556 epoxy compared with Aquabond 520 matrix due to the lowest amount of bonding strength. The brittle mode of fracture can be observed clearly in LY556 epoxy matrix. However, in Aquabond 520 matrix due to the elastic nature, the ductile mode failure is observed in the matrix.

Similarly, the debonding of matrix with reinforcement is more in LY556 epoxy compared to the Aquabond 520 matrix that is shown in Fig. 12b and e. This may be due to the lowest amount of covalent bonding of LY556 epoxy matrix with glass fiber. Figure 12c and f shows the fiber fractures in both composites. During the torsional loading, due to the winding nature of the fiber mat, one end of the fiber is wound, while the other end is unwound along the direction of rotation.

Conclusion

A glass fiber-reinforced polymer (GFRP) composite rod with different matrices (LY556 and Aquabond 520) fabricated by the VARTM method and with the concentric arrangement

of fibers to the axis was used to identify the various failure modes during the torsional test. The observed AE signals were analyzed using time domain, frequency domain and DWPT methods. The following observations are made from the AE analysis.

GFRP rod could be fabricated successfully using the VARTM method. The cylindrical knurling surface grippers gave the best gripping force for holding the specimen during testing without damaging the surface. Due to the concentric arrangement of fibers, the winding and unwinding of fibers took place along the direction of torsional load. From the time domain analysis of AE signals, the high-amplitude and high-variance signals indicated the lack of bonding between the fiber and matrix in the case of Aquabond 520 composite. The peak AE_{RMS} and AE energy were observed at an angle between 5° and 15º in the LY556 epoxy composite. However, in Aquabond 520, it was observed at the angle between 20° and 25º due to its elastic nature, indicating the initiation of failure and the torsional rigidity of materials.

From the FFT, the dominant frequency was observed from the peak amplitude in various frequency ranges and it was correlated with the various failure modes of the composite. For LY556 epoxy matrix, it was 85.459, 141.168 and 300.329 kHz, while in the case of Aquabond 520 matrix, 48.834, 87.901 and 302.77 kHz indicated the failure that occurred in the form of matrix cracking, debonding and fiber fracture, respectively. The discrete wavelet packet transform (DWPT) method was used to determine the physical damage for different FRP composite rods and three types of failure were identified. The observed signals were accumulated in various frequency bands such as 62.5–125 kHz, 125–250 kHz and 250–375 kHz irrespective of the types of matrix, which indicated to three different failure modes. However, due to the elastic nature of Aquabond 520 matrix, propagated AE signals were observed within the matrix, which reduced the amplitude of peak frequencies.

According to the above results, it is clear that the frequency ranges of the FFT obtained correspond to the frequency range of DWPT signal breakdown one hundred percent. Finally, it can be seen that the GFRP composite of the Aquabond 520 matrix has a lower torsional resistance to transfer the load and withstand the applied torsional loads.

Data availability Data sets generated during the current study are available from the corresponding author on reasonable request.

References

1. Ahmadi MS, Johari MS, Sadighi M, Esfandeh M (2009) An experimental study on mechanical properties of GFRP braid-pultruded composite rods. EXPRESS Polym Lett 9:560–568
2. El-Assal AM, Khashaba UA (2007) Fatigue analysis of unidirectional GFRP composites under combined bending and torsional loads. Compos Struct 79:599–605
3. Wang X, Wang Z, Wu Z, Cheng F (2014) Shear behavior of basalt fiber reinforced polymer (FRP) and hybrid FRP rods as shear resistance members. Constr Build Mater 73:781–789
4. Quaresimin M, Susmel L, Talreja R (2010) Fatigue behaviour and life assessment of composite laminates under multiaxial loadings. Int J Fatigue 32:2–16
5. Demircan G, Kisa M, Ozen M, Aktas B (2020) Surface-modified alumina nanoparticles-filled aramid fiber-reinforced epoxy nanocomposites: preparation and mechanical properties. Iran Polym J 29:253–264
6. Özen M, Demircan G, Kisa M, İlik Z (2019) Investigation of usability of waste textile fabrics in composites. Emerg Mater Res 9:18–23
7. Talib AA, Ali A, Badie MA, Lah NA, Golestaneh AF (2010) Developing a hybrid, carbon/glass fiber-reinforced, epoxy composite automotive drive shaft. Mater Des 31:514–521
8. Sevkat E, Tumer H (2013) Residual torsional properties of composite shafts subjected to impact loadings. Mater Des 51:956–967
9. Soykok IF, Tas H, Ozdemir O, Kandas H (2021) Effect of drop weight impact on the torsional-loading behavior of filament wound and prepreg-wrapped composite tubes. Polym Polym Compos 29:617–628
10. Capela C, Ferreira JA, Febra T, Costa JD (2015) Fatigue strength of tubular carbon fibre composites under bending/torsion loading. Int J Fatigue 70:216–222
11. Taşdelen ME, Keleştemur MH, Şevkat E (2016) Torsional behaviour and finite element analysis of the hybrid laminated composite shafts: comparison of VARTM with vacuum bagging manufacturing method. Adv Mater Sci Eng 1:2016
12. Tariq M, Nisar S, Shah A, Akbar S, Khan MA, Khan SZ (2018) Effect of hybrid reinforcement on the performance of filament wound hollow shaft. Compos Struct 184:378–387
13. Arumugam V, Shankar RN, Sridhar BT, Stanley AJ (2010) Ultimate strength prediction of carbon/epoxy tensile specimens from acoustic emission data. J Mater Sci Technol 26:725–729
14. Kakakasery J, Arumugam V, Rauf KA, Bull D, Chambers AR, Scarponi C, Santulli C (2015) Cure cycle effect on impact resistance under elevated temperatures in carbon prepreg laminates investigated using acoustic emission. Compos B 75:298–306
15. Kosmann N, Karsten JM, Schuett M, Schulte K, Fiedler B (2015) Determining the effect of voids in GFRP on the damage behaviour under compression loading using acoustic emission. Compos B 70:184–188
16. Roundi W, El Mahi A, El Gharad A, Rebiere JL (2018) Acoustic emission monitoring of damage progression in glass/epoxy composites during static and fatigue tensile tests. Appl Acous 132:124–134
17. Hao W, Yuan Z, Tang C, Zhang L, Zhao G, Luo Y (2019) Acoustic emission monitoring of damage progression in 3D braiding composite shafts during torsional tests. Compos Struct 208:141–149
18. Karimi NZ, Minak G, Kianfar P (2015) Analysis of damage mechanisms in drilling of composite materials by acoustic emission. Compos Struct 131:107–114

19. Prakash M, Kanthababu M, Rajurkar KP (2015) Investigations on the effects of tool wear on chip formation mechanism and chip morphology using acoustic emission signal in the microendmilling of aluminum alloy. IntJ Adv Manuf Technol 77:1499–1511
20. Bak KM, KalaiChelvan K, Vijayaraghavan GK, Sridhar BT (2013) Acoustic emission wavelet transform on adhesively bonded single-lap joints of composite laminate during tensile test. J Reinf Plast Compos 32:87–95
21. Beheshtizadeh N, Mostafapour A, Davoodi S (2019) Three-point bending test of glass/epoxy composite health monitoring by acoustic emission. Alex Eng J 58:567–578
22. Rishikesan V, Chaturvedi B, Arunachalam N (2021) Characterization of drilling-induced damage in GFRP honeycomb sandwich composites using acoustic emission. Procedia Manuf 53:664–672
23. Duntschew J, Eschelbacher S, Schluchter I, Möhring HC (2021) Discrete wavelet transformation as a tool for analysing the borehole quality when drilling carbon fibre reinforced plastic aluminium stack material. J Mach Eng 2021:21